Mass Transfer and Drag Coefficients of Bubbles Rising in Dilute Aqueous Solutions

DELMAR R. RAYMOND and STEFAN A. ZIEMINSKI

University of Maine, Orono, Maine

The effects of aliphatic alcohols on mass transfer and drag coefficients of a carbon dioxide bubble were investigated in very dilute aqueous solutions. A high speed photography technique provided an almost continuous record of the bubble volume, shape, and oscillation, as related to the height of the bubble in the liquid and the time elapsed from the moment of its release. The results showed that the concentration, molecular size, and structure of the investigated alcohols have a pronounced effect on mass transfer as well as drag coefficients of the rising bubble. The significance of these effects with respect to idealized models of a highly circulating bubble and a solid sphere was considered, and a functional relationship was found to exist. This relationship may be applied to systems more complex than a single bubble.

Minute quantities of some surface-active substances may exert profound and manifold effects on the behavior of gas bubbles in water. Garner and Haycock (*1*) found that these substances can decrease circulation, which, according to Timson and Dunn (*2*), may reduce the rate of mass transfer from rising bubbles. Griffith (*3*) as well as Gorodetskaya (*4*) noted that these substances also decrease the velocity of rise.

An interesting effect of surfactants is the decrease in the degree of coalescence noted in aqueous solutions of some fatty alcohols and acids at concentrations of only a few parts per million. This reduced coalescence reported by Zieminski (*5*) can so increase the surface area of transfer that, even with a lower transfer coefficient, the mass transfer rate can be substantially improved in a multiple bubble system. The action of these substances in gas-liquid dispersions is complicated by the fact that, when the frequency of bubble formation is high and new surfaces are formed at a high rate, surface equilibrium may not necessarily be established. Consequently, the concentration of the adsorbate at the interface would vary with time (Addison *6* to *11*), and its effect would become time dependent (*5*).

The transfer of a gas to a liquid has been extensively studied over a wide range of experimental conditions and in a variety of systems. Baird and Davidson (*12*), Ledig (*13*), Bogdandy (*14*), and others (*15* to *17*) are among those who have studied single bubbles, while Cullen and Davidson (*18*), Baars (*19*), and Zieminski (*5*, *20*) have concerned themselves with slightly more complicated systems. Rosenberg (*21*), Haberman and Morton (*22*), Miyagi (*23*), and Levich (*24*) investigated the hydrodynamic characteristics of rising bubbles.

Although all these studies have definitely contributed to the better understanding of the process of mass transfer, they deal for the most part with pure liquid systems or systems where the concentration of the surface-active agent is relatively high. Unfortunately, very little work has been done on the effects of the structural and other chemical characteristics of these substances in gas liquid dispersions at very low solute concentrations. It is at these very low concentrations that the most anomalous surface behavior occurs (*6* to *11*, *25* to *30*).

Besides its theoretical aspects, the problem is of practical interest in the general area of gas-liquid dispersions. The decrease in density produced by dispersion of a gas in a liquid constitutes the principle of operation of air lifts and mammoth pumps. A local decrease in hydrostatic head caused by introduction of air into liquids has been found to be an efficient method of mixing large bodies of water. In chemical engineering practice, dispersing of gases in liquids is of importance in many gas absorption processes, such as industrial fermentations and waste treatment by bio-oxidation. The economy of these processes depends, among other things, on the size of the bubbles, their shape, velocity of rise, mass transfer coefficient, and coalescence. All these factors are, in turn, affected by the presence of small quantities of surface active impurities.

In this work a systematic study was made of the effects of some members of a homologous series of aliphatic alcohols on the mass transfer and drag coefficients of carbon dioxide bubbles rising freely in a dilute solution (1 to 50 ppm.) of the investigated substances. It was expected that such an investigation would aid in the determination of

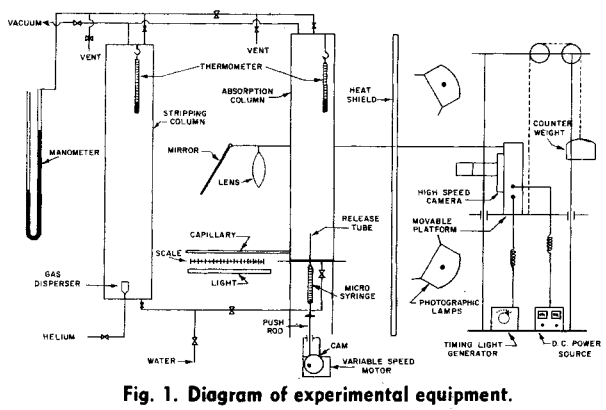

Fig. 1. Diagram of experimental equipment.

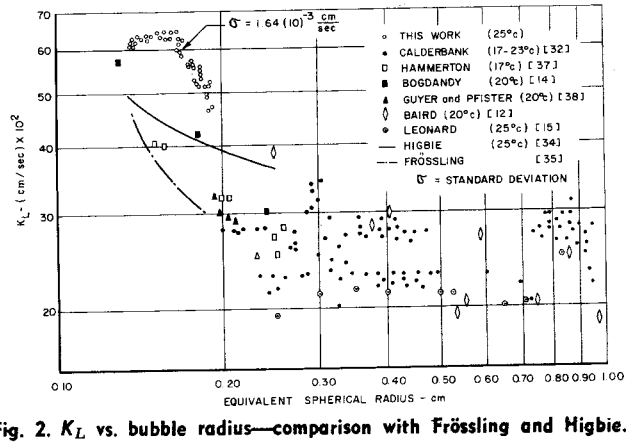

Fig. 2. K_L vs. bubble radius—comparison with Frössling and Higbie.

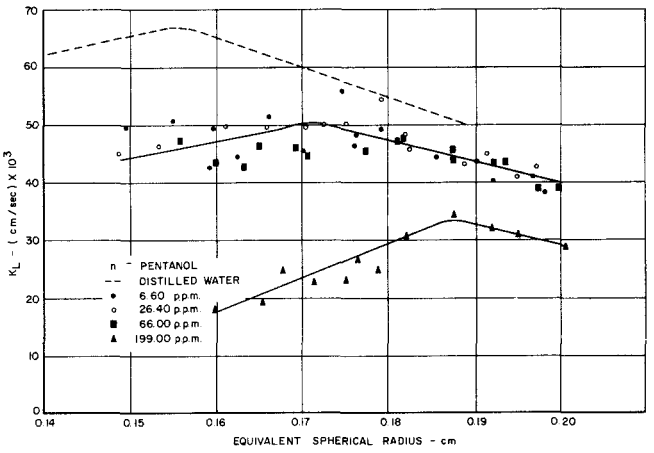

Fig. 3. K_L vs. bubble radius (*n*-pentanol).

the interdependence of these quantities as well as of the magnitude of their effects. To avoid secondary effects caused by interaction of bubbles, only a single bubble was studied.

EXPERIMENTAL PROCEDURE

By means of high speed photography the motion of the bubble was followed simultaneously with the changes in volume, as indicated by the capillary of a dilatometer. In this way an almost continuous record was obtained of the bubble volume, shape, and oscillation as related to the height of the bubble in the liquid and the time elapsed from the moment of release.

Apparatus

The experimental apparatus (Figure 1) consisted of stripping and absorption columns made of plexiglass. The water was twice distilled in a Barnstead borosilicate glass redistiller, stripped from dissolved gases by means of helium under a vacuum, and then introduced into the adsorption column. The column was completely filled with water. A bubble of 99.3% pure carbon dioxide was then introduced at the bottom of the column by means of a specially designed release system.

Motion of the bubble was followed by hand control of a Hycam (Model K1001) high speed camera mounted on a well-balanced movable platform. Attached to the platform was a horizontal bar carrying at its end a reflector and lens to enable photographing of the capillary dilatometer protruding from the bottom of the absorption column. This arrangement made it possible to obtain at every 0.001 sec. pictures of both a bubble and the corresponding position of the meniscus in the dilatometer.

Volume was measured by use of the capillary dilatometer which constituted the only opening to the atmosphere. The shape of the bubble was obtained directly from the high speed photographs and, in the range of bubble sizes studied, was approximated by an oblate spheroid or in some cases a sphere (*2, 24, 31, 32*). Also known from the photographs was the position of the bubble in the column because lines indicating height above the release point were placed on the absorption column. Bubble age was obtained from a series of timed exposures placed on the edge of each film by a calibrated electronic timing device, and the surface area was calculated from the known bubble volume, dimension measurements from the photographs, and the assumption of a geometric shape. Many surface area measurements at each position of the bubble were available due to the speed at which the film was exposed (approximately 1000 frames/sec.).

CALCULATION PROCEDURE

The rate equation for mass transfer from a bubble to the surrounding liquid may be expressed by

$$-\frac{dn}{dt} = K_L A\,(C_0 - C_L) \qquad (1)$$

At any given time the pressure of a rising gas bubble can be related to its volume by

$$PV = n\,R\,T \qquad (2)$$

Equations (1) and (2) may be combined and, if isothermal conditions are assumed, the result is

$$-\frac{1}{RT}\frac{d}{dt}(PV) = K_L A\,(C_0 - C_L)$$

As the water was originally stripped of all absorbed gases, C_L was taken as zero. In very dilute solutions C_0 can be expressed by *Henry's Law* as

$$C_0 = H\,P \qquad (4)$$

The actual pressure experienced by the bubble at any point in the column was represented by

$$P = P_B - \Pi \qquad (5)$$

Assuming negligible surface tension effects and an open system, the pressure inside a stationary and insoluble bubble depends only on the barometric pressure and on the height of the bubble in the column of liquid. Associated with this work is a change in pressure inside the bubble, the magnitude of which depends, in a given system, on the rate of any corresponding volume change and on the position of the bubble in the column. This information was experimentally determined from the volume changes of an insoluble (helium) bubble during its ascent and was then used to estimate Π in Equation (5).

Combining Equations (3), (4), and (5) yields

$$K_L = \frac{1}{RTAH}\left[\frac{V}{P_B - \Pi}\left(\frac{d\Pi}{dt}\right) - \frac{dV}{dt}\right] \qquad (6)$$

Direct measurement of the capillary displacement corrected for the effects of temperature and the water film in the capillary gave the bubble volume. This volume was plotted against the corresponding time determined from the exposure marks of the timing light generator. The rate of volume change of the bubble was then obtained from this curve.

The surface area corresponding to a given bubble volume was calculated from the relationship

$$A = 1.50\frac{V}{b} + 3.14\frac{b^2}{\alpha}\log_e\frac{1+\alpha}{1-\alpha} \qquad (7)$$

where α is expressed in terms of its volume and the minor semiaxis:

$$\alpha = \left(1 - 4.19\frac{b^3}{V}\right)^{1/2} \qquad (8)$$

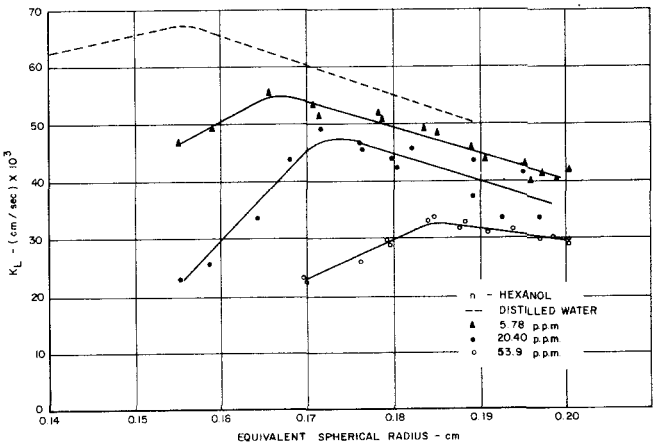

Fig. 4. K_L vs. bubble radius (*n*-hexanol).

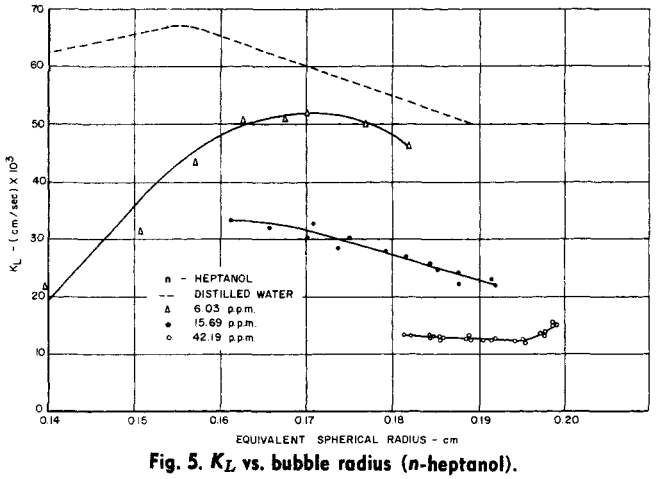

Fig. 5. K_L vs. bubble radius (*n*-heptanol).

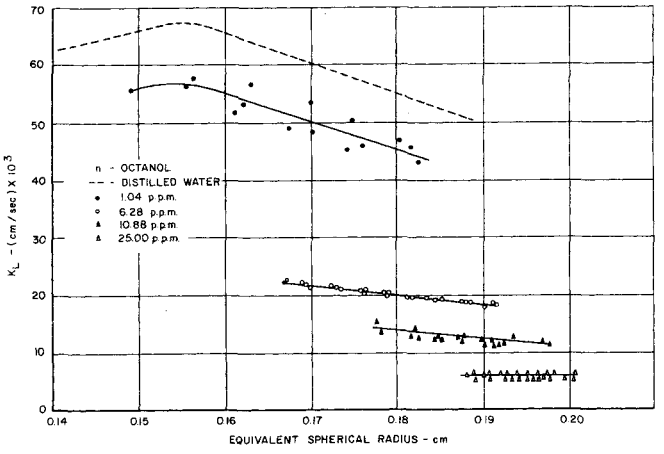

Fig. 6. K_L vs. bubble radius (*n*-octanol).

The major axis of the oblate spheroid was eliminated by means of

$$V = \frac{4}{3}\pi a^2 b \tag{9}$$

Equation (7) simplified the analysis of the photographic results by reducing the number of necessary measurements and at the same time took advantage of the measurable quantity V (33).

The drag coefficient and the Reynolds number were calculated according to the expressions (*1*, *22*)

$$C_D = \frac{8}{3}\frac{gb}{u^2} \tag{10}$$

and

$$N_{Re} = \frac{2a\rho_L u}{\mu_L} \tag{11}$$

RESULTS AND DISCUSSION

Distilled Water Tests

Figure 2 gives the results of gas absorption tests conducted under analogous conditions, as well as the results obtained from the equations of Higbie (*34*) and Frössling (*35*). It relates the instantaneous mass transfer coefficient to the equivalent bubble radius for carbon dioxide bubbles in distilled water. Although most of previously published data lies in the range of bubble radii of 0.20 cm. and higher, the data of the present work fall between bubble radii from 0.13 to 0.20 cm. and pass through a definite maximum. The accuracy of the procedure is indicated by the standard deviation shown in the graph.

Rosenberg (*21*), Levich (*24*), Miyagi (*23*), and others (*4, 14, 22, 33, 31*) found that, as the Reynolds number decreases, the path of the bubble changes from spiral to linear. According to Levich (*24*), this transition occurs at N_{Re} close to 700, corresponding to bubble radii of 0.10 to 0.15 cm. and is accompanied by a change from a spheroidal to a spherical shape. The velocity of rise in this range of diameters is nearly independent of the bubble size and amounts to 28 to 30 cm./sec. (*21, 24, 36*). It is believed that the maximum, Figure 2, may be a result of this shape transition, for a maximum value of K_L was observed at an equivalent bubble radius of 0.155 cm. ($N_{Re} \approx$ 750). Hammerton and Garner (*37*) observed a similar maximum at bubble radii of approximately 0.15 cm.

Also of interest are the somewhat higher values of K_L (Figure 2) compared with those of other authors. It should be noted that these tests were conducted at 25°C. and with bubble sizes not thoroughly investigated. The effect of temperature, although small for larger bubbles (> 0.6 cm. diam.), becomes increasingly important for smaller bubbles above 17°C., rising to about 3%/°C. for bubble sizes studied in this work (*37, 39*).

The method and speed of bubble release also drastically affected the results, and an extensive investigation was undertaken to determine the optimum release conditions (*33*). Bubble release conditions alone may account for some of the scatter of data experienced by other authors.

The theoretical relationships of Higbie (*34*) and Frössling (*35*) exhibit a negative slope that agrees with the reported results for bubbles above a radius of 0.15 cm. At larger radii the experimental values agree well with the theoretical values of Higbie, but deviate considerably below a radius of 0.20 cm. Because the bubbles in this latter region are close to the critical size noted by Levich (*24*), a decrease in circulation makes it doubtful that the Higbie model applies. These observations are in agreement also with the results of Bogdandy et al. (*14*), which show that for smaller bubbles (radius < 0.02 cm.) the experimental values approach those of Krischer and Loos (*40*) for solid spheres. Lochiel (*41*), Gorring and Katz (*42*), and others (*22, 24*) have noticed a change in behavior of the drag coefficient at a Reynolds number of about 750. This change is believed to be due to an alteration in flow characteristics because of the transition from a spherical to a spheroidal shape.

Tests in Dilute Alcohol Solutions

The addition of any surface-active substance to a water-bubble system would be expected to cause considerable alterations in the flow behavior as well as the transfer of gas into the liquid medium. Higbie (*34*), Lewis and Whitman (*43*), Danckwerts (*44*), and others (*45* to *47*) formulated theories to explain mass transfer phenomena in systems of varying complexity, but all these theories assume that the gas-liquid interface offers no resistance to gas absorption. Whether or not surfactants upset this assumption is not clear. What is clear is that even in extremely dilute solutions (< 1 ppm.) these substances have a pronounced effect on both the hydrodynamic behavior and on the rate of mass transfer from the rising gas bubbles (*4, 5*). The question is are these effects separate consequences of some yet unknown phenomena or are they dependent upon each other.

The previous discussion of bubble behavior in distilled water revealed that the maximum (radius of 0.155 cm.) of the K_L curve might be explained by the transition in the shape of the bubble. Following the same line of reasoning, it is possible to examine the effects of some alco-

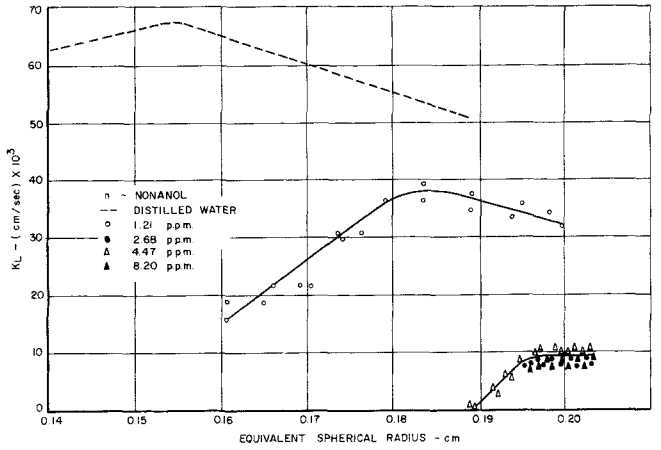

Fig. 7. K_L vs. bubble radius (*n*-nonanol).

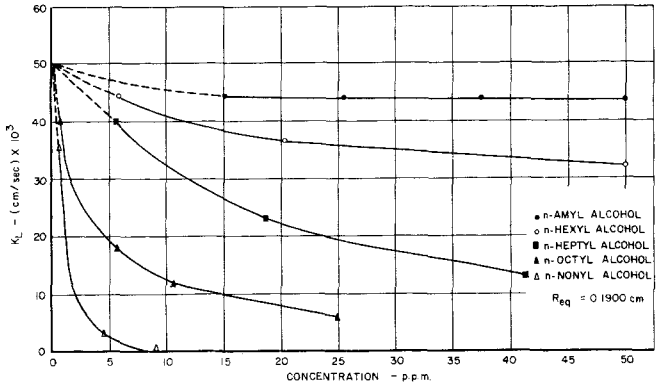

Fig. 8. K_L vs. concentration at (R_{eq} = 0.1900 cm.).

hols on the K_L vs. $R_{eq.}$ relationship.

Surface-active substances have been observed to lower the terminal velocity of bubbles (*3, 4, 24*), increase the drag at a given bubble radius (*24*), cause bubbles to be more spherical than those in water at the same radius (*24*), and decrease interfacial as well as internal turbulence (*24, 37, 48, 49*). The combination of these effects should result in the change from spheroidal to spherical bubbles occurring at a larger radius in the presence of a surface-active solute than in distilled water. The radius at which this transition occurs should depend upon the concentration and the surface activity of the substance.

In Figures 3 through 7 a shift in the K_L curves can be observed in all but one case. For *n*-pentanol the magnitude of the coefficient is relatively unaffected until the concentration exceeds 66 ppm. With the higher alcohols, however, a much lower concentration is capable of shifting the curves drastically. Also at a given concentration there is a trend of decreasing K_L values with increase of the hydrophobic chain length. For *n*-octanol, the range of bubble diameters was not sufficient to record the transition points at all concentrations, while for *n*-nonanol a greater part of the path was more typical of a sphere than a spheroid. Thus alcohol concentration and, in most cases, chain length may be said to have a considerable lowering effect on the mass transfer coefficient.

The more interesting correlation between the mass transfer coefficient and concentration-utilizing carbon chain length as a third parameter could have been constructed from the data in at least two different ways. The integral average of the coefficient over the time of the event could have been taken and this value plotted against concentration, or a bubble radius common to all concentrations might have been selected. Because previous results indicate some dependence of the coefficient on the shape of the bubble and because this shape is a function of bubble radius as well as concentration and chain length, the latter relationship was chosen. A bubble radius of 0.1900 cm. was selected, for all concentrations and chain lengths included this value. Any other choice of radius might have been used, however, with similar results.

Figure 8 shows that with increased concentration of alcohol the mass transfer coefficient drops sharply in the region of low concentration (0 to 5 ppm.) and then gradually levels off. The magnitude of this drop increases with the chain length of the alcohol. At a concentration of about 5 ppm. the amyl alcohol showed a drop of about 5%, while under the same conditions the nonyl alcohol reduced the coefficient by 90%.

To determine the effect of molecular structure, three isomers of straight chain alcohols were selected. Each had the hydroxyl group located at the number four carbon atom. Figures 9, 10, and 11 show the relationship between the mass transfer coefficient and the equivalent bubble radius for 4-heptanol, 4-octanol, and 4-nonanol, respectively, at various concentrations. The general shape of the curves is very similar to those of the straight chain alcohols. A definite maximum occurs in nearly all cases which again appears to depend upon alcohol concentration and hydrophobic chain length. Sufficient data were not available in all cases to record the change in slope.

The most significant difference between the results of the straight chain alcohols and their isomers is the relative location of the maxima for different concentrations of any

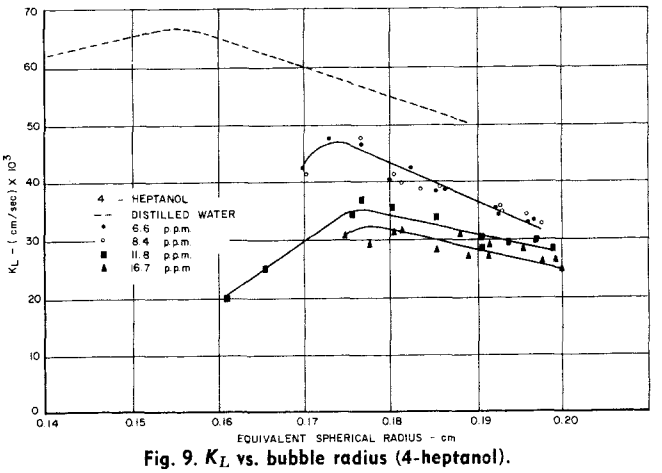

Fig. 9. K_L vs. bubble radius (4-heptanol).

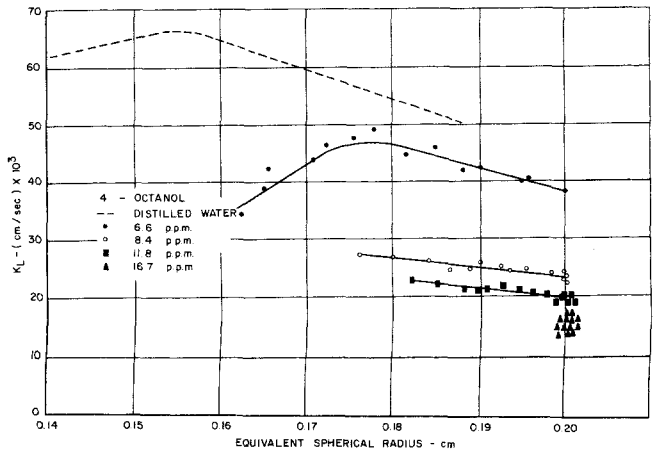

Fig. 10. K_L vs. bubble radius (4-octanol).

one alcohol. It was pointed out that for the normal alcohols there was a shift of the maximum, which is not as noticeable with the isomers if it is present at all.

A better picture (Figure 12) of the effects of molecular structure can be obtained by relating the mass transfer coefficient to the concentration at a constant equivalent bubble radius (0.1900 cm.) For heptanol there is essentially no difference between the isomers. This is in agreement with the results obtained with isomers of butyl alcohol (5) where no change was observed in their effects on mass transfer coefficient. For octanol and nonanol, however, the mass transfer coefficient for the normal alcohols falls well below those for their isomers at the same concentration. This behavior may be due to the higher solubility of the isomers and to the greater proximity of their centers of hydrophobic and hydrophilic attraction to the center of the molecule, characteristics that may make it less able to impart a stabilizing effect to the surface. Whatever the mechanism involved, it should depend on the type and concentration of the adsorbate molecules at the gas-liquid interface and therefore on the rate of transfer of the solute to the bubble surface.

Addison found (6 to 8, 50) that the velocity of migration of straight chain alcohols increases with the length of the carbon chain, and therefore for the same concentration the rate of accumulation is higher for alcohols of larger molecular size. Hence the higher the alcohol the more pronounced its depressing effect on the mass transfer coefficient.

This decrease of the coefficient appears to be more of a hydrodynamic than of a surface-resistance nature (51). Garner and Haycock (1) as well as Baird and Davidson (12) noticed that the presence of surface-active substances decreases circulation and thus lowers the rate of mass transfer because of decreased surface disturbance. It is possible that this lowering of circulation is due to absorption of the alcohol molecules and attraction of their polar groups of water. Action of this kind should increase the stability of the layer of water adjacent to the bubble. This effect can be expected to be more pronounced the higher the molecular weight of the alcohol, because the attraction between carbon chains of the adsorbate molecules increases with the chain length (6).

Furthermore, it has been suggested that in solutions of surface-active substances the motion of a bubble sets up surface tension gradients at the interface (2, 3). If this is correct, it seems reasonable to assume that an increase in the concentration or chain length would increase the magnitude, and thus the rigidity, of the surface and the drag coefficient.

The drag coefficient of rising bubbles has been studied extensively in water by Rosenberg (21), Haberman and Morton (22), and others (14, 24, 52). However, except for the studies of Lochiel (41), Griffith (3), and Gorodetskaya (4), very few investigations have been made of the drag on a bubble rising freely in very dilute solution of a surfactant. In order to throw more light on such action, drag coefficients were determined under conditions analogous to those of the mass transfer tests.

Figures 13 through 16 show the relationship between Reynolds number and drag coefficient for solutions of *n*-heptanol, *n*-octanol, 4-heptanol, and 4-octanol respectively. Since all bubbles remained in the experimental column for approximately the same time, the effect of the alcohols on the rate of gas absorption is no doubt responsible for the different ranges of Reynolds numbers.

In all cases where data were available near $N_{Re} = 750$ (transition point of water), the addition of an alcohol resulted in a higher drag coefficient. The magnitude of this difference increased with increased solute concentration. Moreover, at higher Reynolds numbers the values of the drag coefficient appear to be very close to those for distilled water, especially at the lower concentrations of solute. This increase in drag coefficient near $N_{Re} = 750$ smooths out the very definite inflection noted in the case of distilled water and is in agreement with the results of Haberman and Morton (22). This behavior may be due to the surface tension gradients noted by Griffith (3) and Timson and Dunn (2), or it may be a result of the building in of alcohol molecules at the water surface, as suggested by Kipling (30), Franks and Ives (29), and Dunicz (53), it may also be a combination of both. Whatever the reason, the effect appears to be a function of solute concentration and length of the carbon chain.

To demonstrate the effects of these alcohols, the drag coefficient was plotted against the solute concentration at a selected Reynolds number ($N_{Re} = 750$). Figure 17 shows that the drag coefficient levels off after a certain concentration is reached. It is apparent that the longer the carbon chain, the lower the concentration necessary to reach this plateau. With regard to the shorter carbon chains, 4-heptanol and 4-octanol, there is very little effect due to the chain structure, but the values of C_D for the 4-nonanol fall well below those of *n*-nonanol. Whatever their origin, the factors affecting the drag of the bubble cease to influence the drag coefficient beyond a certain critical concentration, which varies with chain length and chain structure.

The most striking result is the similarity of behavior of the mass transfer and drag coefficients. Whereas the mass transfer coefficient decreased with increase of the length of the carbon chain, the change in the drag coefficient was found to be nearly identical but in the opposite direction.

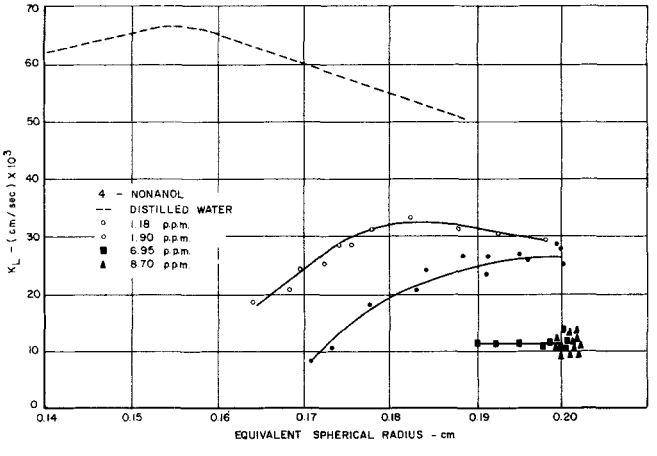

Fig. 11. K_L vs. bubble radius (4-nonanol).

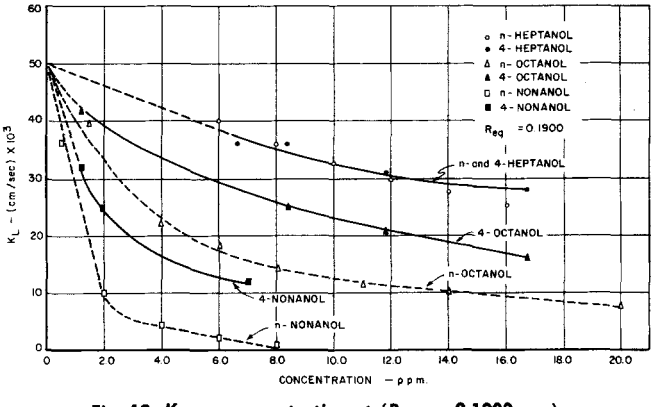

Fig. 12. K_L vs. concentration at (R_{eq} = 0.1900 cm.).

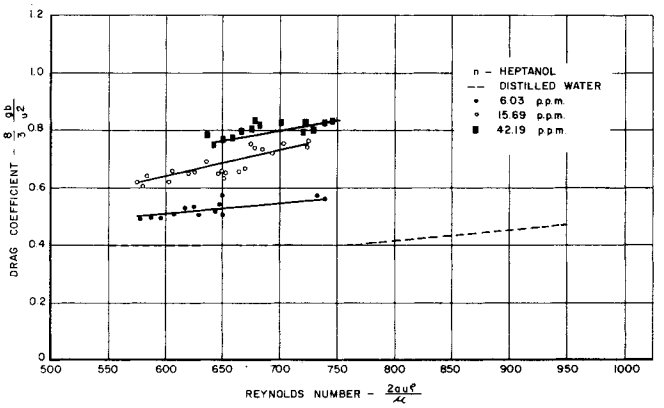

Fig. 13. Drag coefficient vs. N_{Re}, *n*-heptanol.

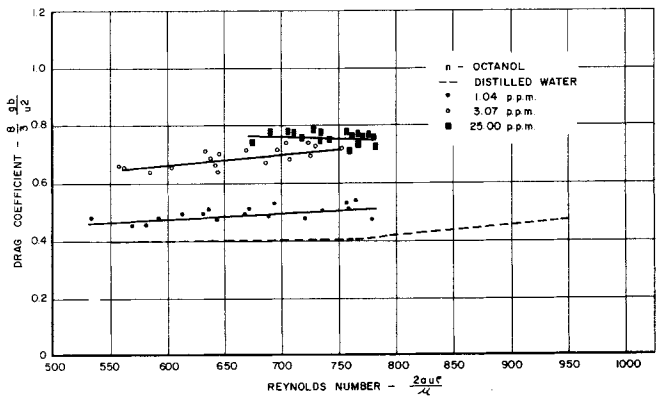

Fig. 14. Drag coefficient vs. N_{Re}, *n*-octanol.

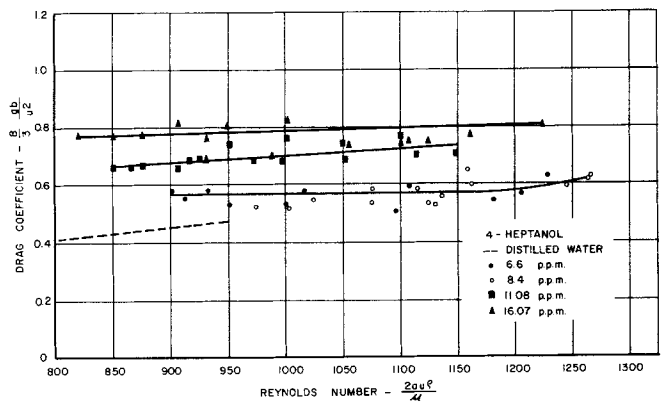

Fig. 15. Drag coefficient vs. N_{Re}, 4-heptanol.

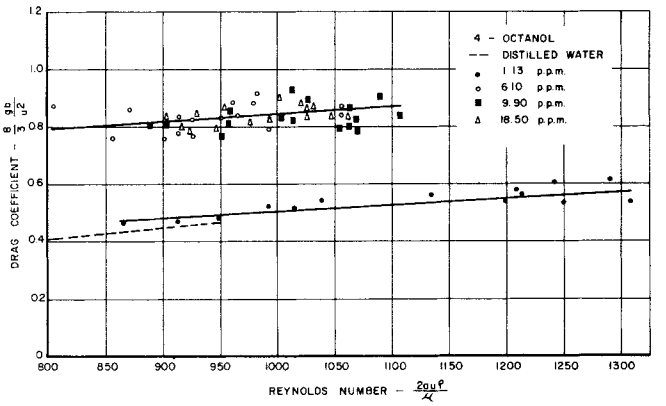

Fig. 16. Drag coefficient vs. N_{Re}, 4-octanol.

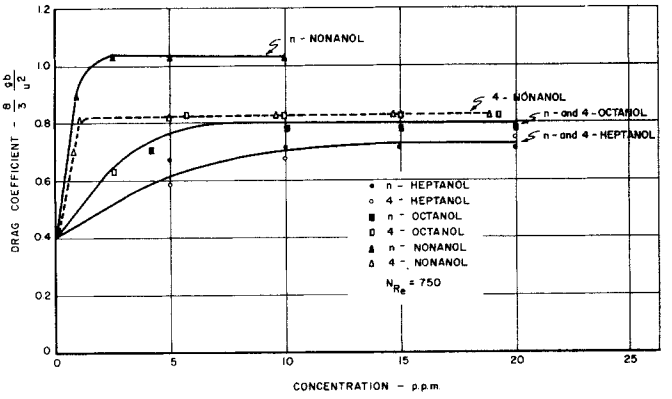

Fig. 17. Drag coefficient vs. concentration at $N_{Re} = 750$.

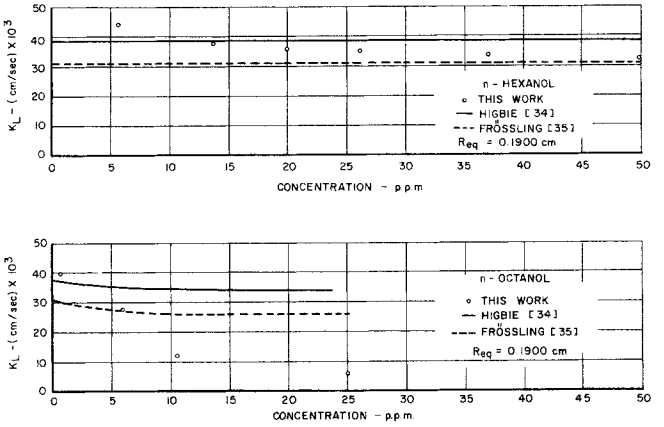

Fig. 18. K_L vs. concentration—comparison with Frössling and Higbie.

It seems logical therefore to assume that the factors that increase the drag coefficient produce an adverse effect on mass transfer and that this behavior is a function of the chain length.

Previous results indicate that bubbles approximating both solid spheres and highly circulating spheroids were present over the range of data studied. It is thus appropriate to examine the limiting cases of mass transfer from solid spheres and circulating bubbles. In the following discussion the K_L for solid spheres was calculated by Frössling (35),

$$K_L = 0.6\frac{D}{R_{eq}}N_{Re}^{0.5}N_{Sc}^{0.333}$$

while the K_L for circulating bubbles was evaluated by Higbie's relationship (34),

$$K_L = 2\,(D/\pi t_e)^{1/2}$$

where t_e is the time required for a bubble to move one bubble diameter.

Experimental results might be expected to fall between the limits set by these two equations, their position depending upon the alcohol concentration and chain length. Such was not the case (Figure 18), although a definite trend is indicated. For example, at low concentrations of alcohol the Higbie relationship comes much closer to predicting the actual value of K_L than does the Frössling expression. At higher concentrations, however, the Frössling equation yields a more accurate result. It is further noticed that the Frössling equation becomes more accurate at a lower concentration for the eight- than for the six-carbon alcohol. This behavior might have been expected, for a bubble rising in distilled water is highly circulating and oscillating throughout most of its ascent. The addition of

alcohol to the water has the effect of damping these oscillations. The higher the concentration or chain length, the sooner this damping occurs within the range of experimental results. When a bubble is behaving similarly to one in distilled water, the Higbie relationship is more accurate, but as the interface becomes more contaminated, the Frössling equation is a better approximation.

This conclusion is somewhat similar to that of Calderbank (*54*) who found that bubbles in water at diameters above 2.5 mm. have greater values of K_L than those below 2.5 mm. He suggests that below this diameter friction drag predominates causing boundary layer flow and Frössling's equation is applicable. Above a diameter of 2.5 mm., however, form drag prevails and the Higbie relationship should be applied.

In Figure 19 the experimental Nusselt numbers are presented as a function of the Reynolds number together with the results of Bogdandy (*14*) for deformed bubbles and those of Krischer and Loos (*40*) for solid spheres. The values for water and for very low concentrations of alcohols are seen to fall close to the experimental values of Bogdandy. As concentration is increased, however, the bubbles behave more and more like solid spheres. At 8.2 ppm. *n*-nonanol, the experimental points are seen to fall on the line of Krischer and Loos. The effect of chain length can also be seen as 10.8 ppm. *n*-octanol yielded much lower N_{Nu} than did *n*-hexanol of the same concentration.

It would appear therefore that the decrease in the rate of mass transfer upon the addition of a surface-active substance is not the result of a surface resistance, but is primarily due to changes in the hydrodynamic characteristics of the system. Thus a functional relationship should exist between the mass transfer and hydrodynamic characteristics and this relationship should be independent of bubble radius, surfactant concentration, and hydrophobic chain length. Consequently a plot of the mass transfer coefficient against a representative hydrodynamic quantity, the drag coefficient, should exhibit some predictable functional relationship.

The solid circles in Figures 20 and 21 represent experimental data for all alcohols investigated at the various concentrations used as well as the values for distilled water. All points fall within a band approximating a straight line except for one cluster in Figure 20 which appears to the lower right of the line. These points were obtained with 8.2 ppm. *n*-nonanol; apparently, as the drag coefficient increases the mass transfer coefficient approaches zero.

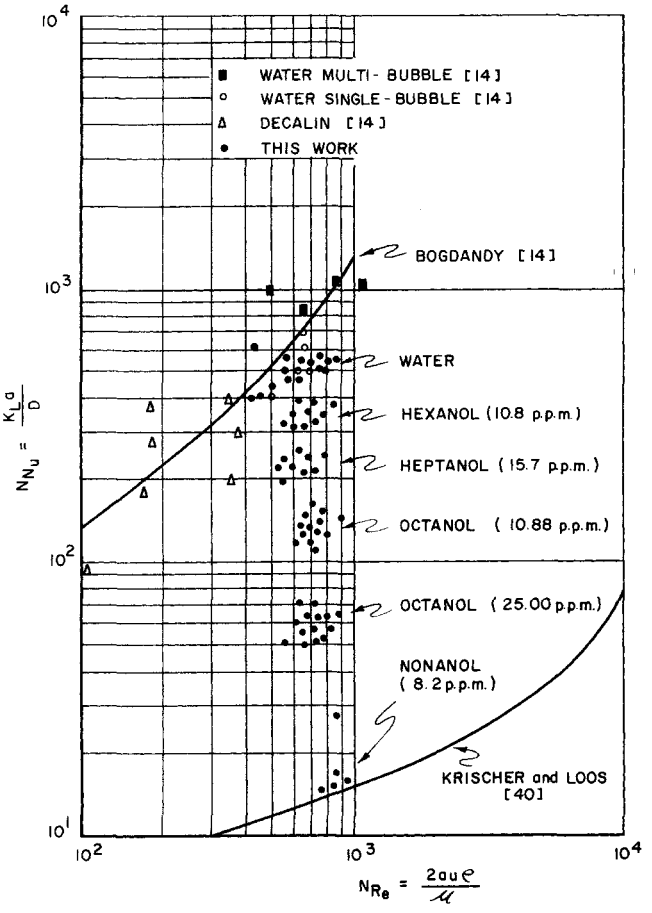

Fig. 19. Nusselt number vs. Reynolds number.

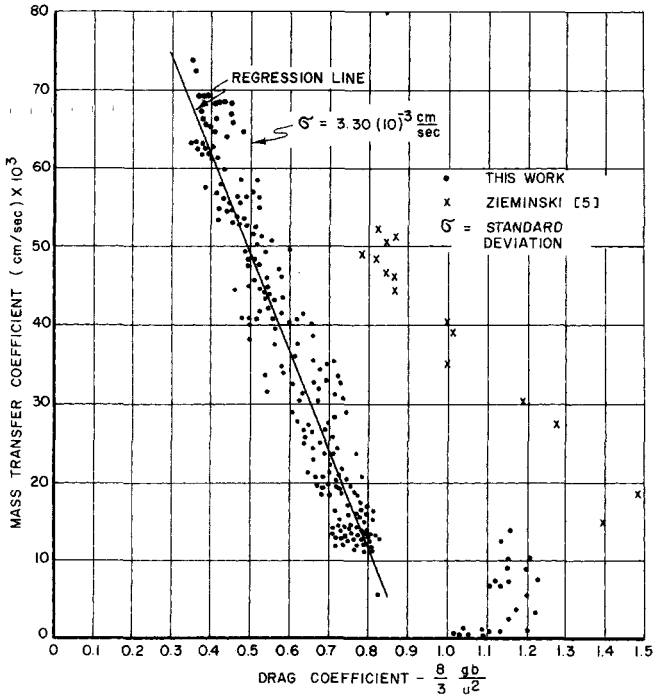

Fig. 20. K_L vs. drag coefficient, normal alcohols.

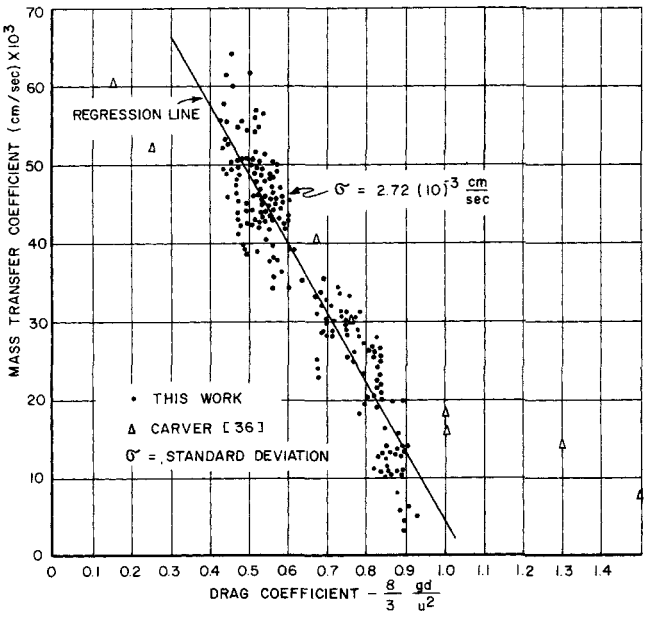

Fig. 21. K_L vs. drag coefficient, isomers.

Therefore, there should exist a point beyond which an increase in C_D will have only very little effect on the value of K_L, and the linear relationship would no longer apply.

Shown in Figure 20 and 21 are the linear regression lines from which the functional relationships for single bubbles were determined. For the straight chain alcohols this relationship was found to be

$$K_L = -0.126\,C_D + 0.1120$$

and for the isomers

$$K_L = -0.089\,C_D + 0.0903$$

There is a small but significant difference between these relationships. It suggests that the relationship is not completely independent of molecular structure. Furthermore, if the transfer coefficient can truly be expressed in terms of the drag coefficient, similar equations should exist regardless of the system used. It should therefore be possible to correlate in a similar manner data taken on systems of a more complex nature than single bubbles.

Figures 20 and 21 indicate also the results of Zieminski (*5*) and Carver (*36*), respectively. The former used a stone disperser and dilute solutions of alcohols, whereas the latter dispersed air into a dilute solution of a detergent using a venturi diffuser. Even in these widely different systems there is a visible relationship between the mass transfer and drag coefficient. It seems, therefore, that the interdependence of C_D and K_L is not restricted to the single-bubble system used in this investigation.

ACKNOWLEDGMENT

This investigation was supported by the U.S. Department of the Interior, Federal Water Pollution Control Administration, Grant: WP 00562-0.4

NOTATION

a = major semiaxis of a spheroid, cm.
A = surface area of bubble, sq.cm.
b = minor semiaxis of a spheroid, cm.
c = conversion factor, 0.9678×10^{-3} atm./cm.
C_D = drag coefficient, $8/3\ gD_b/u^2$
C_L = bulk concentration of gas, g.moles/cc.
C_0 = equilibrium concentration of gas, g.moles/cc.
D = diffusivity of absorbed gas through liquid, sq.cm./sec.
g = gravitational constant, 980 cm./sec.^{2}
h = height of bubble in column measured from column base, cm.
H = Henry's law constant, g.moles/cc. atm.
K_L = overall mass transfer coefficient, g.moles/sq.cm. sec. (g.moles/cc.)
n = g.moles of gas
N_{Nu} = Nusselt number, K_La/D
N_{Re} = Reynolds number, $2au\rho_L/\mu_L$
N_{Sc} = Schmidt number, μ_L/ρ_LD
ppm. = parts per million by volume
P = pressure of gas inside bubble, atm.
P_B = barometric pressure, atm.
R = gas constant, 82.057 atm. cc./g.mole °K.
R_{eq} = equivalent spherical bubble radius, cm.
t = time, sec.
T = temperature, °K.
u = linear velocity of rise of bubble, cm./sec.
V = bubble volume, cc.

Greek Letters

α = eccentricity, $[1 - 4.19(b^3/z)]^{1/2}$
δ = dynamic pressure, atm.
μ_L = liquid viscosity, g./cm. sec.
Π = $hc' + \delta$, atm.
ρ_l = liquid density, g./cc.
σ = standard deviation

LITERATURE CITED

1. Garner, F. H., and P. J. Haycock, *Proc. Roy. Soc.*, **252**, 457 (1959).
2. Timson, W., and C. G. Dunn, *Ind. Eng. Chem.*, **52**, 799 (1960).
3. Griffith, R. M., *Chem. Eng. Sci.*, **17**, 1057 (1962).
4. Gorodetskaya, A. V., *J. Phys. Chem. (U.S.S.R.)*, **23**, 71 (1949).
5. Zieminski, S. A., M. M. Caron, and R. B. Blackmore, *Ind. Eng. Chem. Fundamentals*, **6**, 233 (1967).
6. Addison, C. C., *J. Chem. Soc.*, 256 (1944).
7. ———, *ibid.*, 480 (1944).
8. ———, *ibid.*, 98 (1945).
9. ——— and D. Litherland, *ibid.*, 1143 (1953).
10. ———, *ibid.*, 1155 (1953).
11. ———, *ibid.*, 1159 (1953).
12. Baird, M. H. I., and J. F. Davidson, *Chem. Eng. Sci.*, **17**, 87 (1962).
13. Ledig, P. J., *Ind. Eng. Chem.*, **16**, 1231 (1924).
14. Bogdandy, L., *Chem. Ingr. Tech.*, **31**, 580 (1959).
15. Leonard, J. H., and G. Houghton, *Chem. Eng. Sci.*, **18**, 133 (1963).
16. Ledig, P. J., and E. R. Weaver, *J. Am. Chem. Soc.*, **46** (1924).
17. Krishnamurth, S., R. Kumar, and R. L. Datta, *Trans. Indian Inst. Chem. Engrs.*, **6**, 22 (1964).
18. Cullen, E. J., and J. F. Davidson, *Chem. Eng. Sci.*, **6**, 49 (1956).
19. Baars, J. K., *J. Inst. Sewage Purification*, **4**, 358 (1955).
20. Zieminski, S. A., C. C. Goodwin, and C. Hill, *Tappi*, **43**, 1029 (1960).
21. Rosenberg, B., *Report 727*, Navy Dept., Washington, D. C. (1950).
22. Haberman, W. L., and R. K. Morton, *Report 802*, Navy Dept., Washington, D. C. (1953).
23. Miyagi, O., *Phil. Mag.*, **50**, 133 (1925).
24. Levich, V. G., "Physicochemical Hydrodynamics," Ch. 8, Prentice Hall, New Jersey (1962).
25. Defay, R., and J. Hommelen, *J. Colloid Sci.*, **14**, 411 (1959).
26. Ward, A. F. H., *Trans. Faraday Soc.*, **42**, 399 (1946).
27. ———, and L. Tordai, *J. Chem. Phys.*, **14**, 453 (1946).
28. Alexander, A. E., *Trans. Faraday Soc.*, **37**, 15 (1941).
29. Franks, F., and D. J. G. Ives, *J. Chem. Soc.*, 741 (1960).
30. Kipling, J. J., *J. Colloid Sci.*, **18**, 502 (1963).
31. Deindoerfer, F. H., and A. E. Humphrey, *Ferment. Res. Eng.*, **53**, 755 (1961).
32. Calderbank, P. H., and A. C. Lochiel, *Chem. Eng. Sci.*, **19**, 485 (1964).
33. Zieminski, S. A., and D. R. Raymond, *ibid.*, **23**, 17 (1968).
34. Higbie, R., *Trans. Am. Inst. Chem. Engrs.*, **31**, 365 (1935).
35. Frössling, N., *Beitr. Geophysik*, **52**, 170 (1938).
36. Carver, C. E., and A. T. Ippen, *Tech. Rept.* No. 14, U.S. Public Health Project No. G-863 (1955).
37. Hammerton, D., and F. H. Garner, *Trans. Inst. Chem. Engrs.*, **32**, S. 18 (1954).
38. Guyer, A., and X. Pfister, *Helv. Chim. Acta*, **29**, 1173 (1946).
39. Downing, A. L., and G. A. Tuesdale, *J. Appl. Chem.*, **5**, 570 (1955).
40. Krischer, O., and G. Loos, *Chem. Ingr. Tech.*, **30**, 30 (1958).
41. Lochiel, A. C., *Can. J. Chem. Eng.*, **40**, (1965).
42. Gorring, R. L., and D. L. Katz, *AIChE J.*, **8**, 123 (1962).
43. Lewis, W. K., and W. G. Whitman, *Ind. Eng. Chem.*, **16**, 1215 (1924).
44. Danckwerts, P. V., *ibid.*, **46**, 1460 (1951).
45. Perlmutter, D. C., *Chem. Eng. Sci.*, **16**, 287 (1961).
46. Kishinevski, M., *J. Appl. Chem. (U.S.S.R.)* **28**, 881 (1955)

47. Dobbins, W. E., *Intern. Congr. Water Pollution Resources*, London (1962)
48. Goodridge, F., and L. D. Robb, *Ind. Eng. Chem. Fundamentals*, 4, 49 (1965).
49. Davies, J. T., and E. K. Rideal, "Interfacial Phenomena," Ch. 7, Academic Press, New York (1966).
50. Addison, C. C., *J. Chem. Soc.*, 354 (1945).
51. Boxhov, I., and D. Elenkov, *Compt. Rend. Acad. Bulgare. Sci.*, 16, 277 (1963).
52. Garner, F. H., and D. Hammerton, *Chem. Eng. Sci.*, 3, 1 (1954).
53. Dunicz, B. L., *Tech. Rept. No. 951*, U.S. Naval Radiological Defense Laboratory, (Nov. 1965).
54. Calderbank, P. H., *Chem. Engr.*, CE209 (Oct., 1967).

Manuscript received January 21, 1969; revision received May 15, 1969; paper accepted May 19, 1969.

Iterative Methods for Solving Problems in Multicomponent Distillation at the Steady State

D. S. BILLINGSLEY and G. W. BOYNTON

IBM, Houston, Texas

The multicomponent distillation problem is formulated so that unknown compositions do not appear explicitly either in the equilibrium and material balance equations or in the heat balance equations. Use of this formulation in absolute iteration as well as Newton-Raphson iteration is discussed. Other types of staged separation processes may be similarly expressed

Several authors have proposed Newton-Raphson or similar schemes for solving steady state multicomponent distillation problems. Among these are Stainthorp et al. (*11, 12*), Naphtali (*7*), and Greenstadt et al. (*5*). In addition, Newman (*8*) presented a worthwhile scheme for obtaining the temperature profile corresponding to a specified phase flow profile. In these methods the unknown flow rates or mole fractions of individual components enter explicitly into the iterations. When component enthalpies and equilibrium ratios are independent of composition (heats of mixing are neglected), this explicit dependence may be removed, thereby greatly reducing the number of unknowns entering the iterative procedure.

Figure 1 illustrates indexing conventions and some notations. Component enthalpies and equilibrium ratios are assumed to be independent of composition. This assumption imposes no real limitation because nonideal mixtures can be handled as suggested in reference 3. It will be assumed also that each feed stream is completely specified and that the heat duty Q_q of each intercooler and interheater (other than the reboiler and overhead condenser) is specified. The total withdrawal rate of each side-draw, if any, will be specified, and each side-draw will be liquid. For purposes of discussion, a total condenser producing bubble point reflux is employed and any two of the following are specified: internal reflux ratio R, reboiler duty Q_R, bottom product withdrawal rate B, and condenser duty Q_c.

The special algorithm for Gaussian elimination, as applied to tridiagonal matrix equations (see reference 2 or 9), is presumed to be used for solving all such systems otherwise numerical instability will normally result. The reader is referred to Pease (*10*) concerning differentiation of negative powers of matrices.

ITERATION EQUATIONS

Following Ball (*1*), Equation (1) was derived previously (*2*).

$$Z_i^{-1}\ \Omega_i = \Upsilon_i \equiv (v_{iJ}, v_{iJ-1}, \ldots, v_{i1})^T \qquad (1)$$

where

$$\Omega_i = (\omega_{iJ-1}, \omega_{iJ-2}, \ldots, \omega_{i0})^T$$

$$\omega_{ij} = \begin{cases} f_{ij} & \text{if } j \text{ denotes a feed stage} \\ 0 & \text{otherwise} \end{cases}$$